Quantification of the Degradation of Steels Exposed to Liquid Lead-Bismuth Eutectic

C. Schroer, Z. Voß, J. Novotny, J. Konys
Institut für Materialforschung
Programm Nukleare Sicherheitsforschung

Mai 2006

Forschungszentrum Karlsruhe

in der Helmholtz-Gemeinschaft

Wissenschaftliche Berichte

FZKA 7224

Quantification of the Degradation of Steels Exposed to Liquid Lead-Bismuth Eutectic

C. Schroer, Z. Voß, J. Novotny, J. Konys

Institut für Materialforschung

Programm Nukleare Sicherheitsforschung

Forschungszentrum Karlsruhe GmbH, Karlsruhe

2006

Abstract

Metallographic and gravimetric methods of measuring the degradation of steels are introduced and compared, with emphasis on the quantification of oxidation in molten lead-bismuth eutectic (LBE). In future applications of LBE or other molten lead alloys, additions of oxygen should prevent the dissolution of steel constituents in the liquid heavy metal. Therefore, also the amount of steel constituents transferred between the steel (including the oxide scale formed on the surface) and the LBE has to be assessed, in order to evaluate the efficiency of oxygen additions with respect to preventing dissolution of the steel. For testing the methods of quantification, specimens of martensitic steel T91 were exposed for 1500 h to stagnant, oxygen-saturated LBE at 550°C, whereby, applying both metallographic and gravimetric measurements, the recession of the cross-section of sound material deviated by ± 3 µm for a mean value of 11 µm. Although the transfer of steel constituents between the solid phases and the LBE is negligible under the considered exposure conditions, the investigation shows that a gravimetric analysis is most promising for quantifying such a mass transfer. For laboratory experiments on the behaviour of steels in oxygen-containing LBE, it is suggested to make provisions for both metallographic and gravimetric measurements, since both types of methods have specific benefits in the characterisation of the oxidation process.

Kurzfassung

Quantifizierung des Materialverlustes an Stählen nach Auslagerung in flüssigem Blei-Bismut-Eutektikum

Metallographische und gravimetrische Methoden zur Bestimmung des Materialverlustes an Stählen sind hinsichtlich ihrer Eignung zur Quantifizierung der Oxidation in geschmolzenem eutektischen Blei-Bismut (LBE) untersucht worden. Für zukünftige Anwendungen von LBE bzw. anderen, flüssigen Blei-Legierungen soll durch Zugabe von Sauerstoff verhindert werden, dass sich die Stahlbestandteile in der Schwermetallschmelze auflösen. Demnach sind die zwischen dem Stahl (gebildete Oxide eingeschlossen) und dem LBE ausgetauschten Mengen an Stahlbestandteilen ebenfalls zu quantifizieren, um die Effektivität einer Sauerstoffzugabe hinsichtlich der Vermeidung von Stahlauflösung beurteilen zu können. Die Quantifizierungsmethoden sind an Proben aus dem martensitischen Stahl T91, die stehendem, mit Sauerstoff gesättigten LBE bei 550°C ausgesetzt waren (für 1500 h), getestet worden, wobei sich Abweichungen in den gemessenen Querschnittsänderungen von ± 3 µm bei einem Mittelwert von 11 µm ergaben. Obwohl im Falle des beispielhaft betrachteten Korrosionssystems der Übergang von Stahlbestandteilen zwischen den festen Phasen und LBE von untergeordneter Bedeutung ist, zeigen die Ergebnisse dennoch, dass die Analyse mit gravimetrischen Methoden sehr aussichtsreich in Hinblick auf eine Quantifizierung solcher Vorgänge ist. Für Untersuchungen zum Verhalten von Stählen in sauerstoffhaltigem LBE unter Laborbedingungen wird empfohlen sowohl metallographische als auch gravimetrische Messungen vorzusehen, da beide Arten von Methoden spezifische Vorteile bei der Charakterisierung des Oxidationsprozesses bieten.

Table of Contents

1 Introduction

The corrosion behaviour of materials under service conditions in a plant is often complex and, in most cases, only rudimentarily understood on the basis of corrosion mechanisms. Therefore, the measurement of the progress of corrosion up to times which approach the designated service time of the components is necessary for a quantitative determination of the material performance. Mechanistic considerations based on accompanying analyses of corrosion phenomena and modelling of kinetics using the data collected can be helpful to predict the evolution of material degradation with time, but, in general, extrapolation by more than one order of magnitude is not recommended. The quantity which needs to be determined is the loss of sound material, i.e., that part of the initial cross-section which is no longer capable of bearing the different types of loads affecting the material under service conditions.

The specific case considered in this report is the corrosion of steels in liquid lead (Pb) alloys, especially lead-bismuth eutectic (LBE), at temperatures between 500° and 600°C. Unless provision is made to remove oxygen, the traces always present in the fresh melt are sufficient for formation of oxides of chromium (Cr) and iron (Fe), which are the main constituents of the materials to be employed. Due to oxidation processes, the oxygen content of the liquid heavy metal steadily decreases, giving rise to dissolution of steel constituents, especially nickel (Ni) from austenitic steels, when the oxygen content falls below a certain level necessary for stabilising an oxide scale on the steel surface. A viable means of preventing such a dissolving corrosion which starts locally, preferentially at weak points of the oxide scale formed, is to add small amounts of oxygen continuously to the liquid heavy metal, so that a protective oxide scale establishes on the entire steel surface without constituents of the melt, e.g., Pb, being oxidised. When working perfectly, the loss of sound material—or "loss of sound metal" in the case of steels—is then determined by the effects of the small amounts of oxygen, i.e., oxide scale formation and growth, ingress of oxygen into the steel etc. However, there are indications that significant dissolution, e.g., of Fe from steel T91, can also occur through an oxide scale on the steel surface (or parts of the oxide scale are eroded by flowing liquid heavy metal), which needs to be investigated in addition to the quantification of metal loss.[1]

Procedures most commonly used for quantifying the material degradation due to high-temperature corrosion processes rely on measuring either the change in geometric dimensions or the mass change of a sample after a certain exposure time to the corrosive environment.[2,3] Both types of methods are examined in this report with respect to their applicability to the corrosion of steels in oxidising Pb alloys using samples which were exposed to oxygen-containing LBE at 550°C. The pre-exposure measurement of the initial geometric dimensions described is specific for a cylindrical specimen shape employed in this investigation, but the measuring principle can easily be adapted to other geometries.

2 Samples

The methods of quantification of the degradation of steels in oxidising Pb alloys are investigated on specimens of T91, a ferritic/martensitic steel with nominally 9 mass-% Cr and 1 mass-% molybdenum (Mo). The shape of these specimens is a

cylinder of nominal dimensions ∅8×35 mm, with the ends having an internal and external screw-thread (Figure 1). The end with the external thread also has two parallel planar surfaces where a wrench can be used for screwing together and unscrewing the specimens. The convex part of the surface was finished by turning, resulting in a maximum depth of roughness (R_t) around 2 µm (measured on one specimen from the employed batch). The specimen design is the same as used for exposure experiments performed in the CORRIDA loop at the Karlsruhe Lead Laboratory (KALLA).[1]
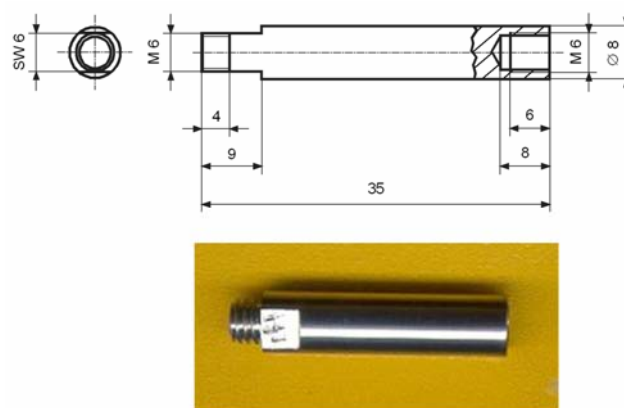
Figure 1 – *Shape of specimens employed in the investigation on methods of quantifying the degradation of steels which were exposed to oxygen-containing LBE. The surface of the specimens was finished by turning.*
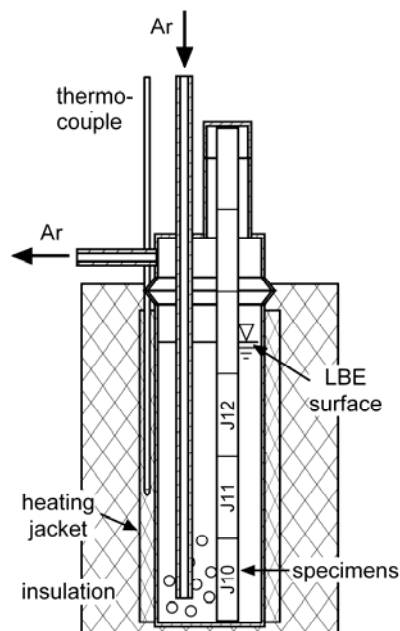
Figure 2 – *Schematic illustration of the apparatus used for the exposure of steel specimens to stagnant oxygen-containing LBE. A small amount of oxygen is steadily introduced into the liquid heavy metal via the impurities in an argon (Ar) stream conducted through the melt.*

2

Corroded specimens were produced in the laboratory apparatus which is schematically shown in Figure 2. The apparatus consists of a capsule made of 17-12 Cr-Ni steel (DIN W.-Nr. 1.4571) which contains the LBE and a rod of five of the specimens described above. This capsule was loaded in an argon (Ar) atmosphere (glovebox), in order to minimise the contamination with oxygen and to prevent excessive oxidation of Pb during the exposure experiment. The small amounts of oxygen necessary to maintain oxidising conditions for the exposed steel were introduced via an Ar stream (>99.9999 vol.-% Ar) conducted through the liquid heavy metal. The temperature was controlled from outside the capsule using a thermocouple which resided between the capsule and a heating jacket.

After 1500 h of exposure at 550°C to stagnant oxidising LBE, the T91 specimens were removed from the capsule. Moderate oxidation of Pb took place at the LBE surface, but, from optical inspection, the three specimens which were completely immersed in the LBE (designated J10, J11 and J12; Figure 2) were not affected by lead oxide (PbO) formation. The outer appearance of these specimens and also the structure of the oxide scale on the steel surface, which was checked using specimen J11 (Figure 3), coincided qualitatively with observations made on the same
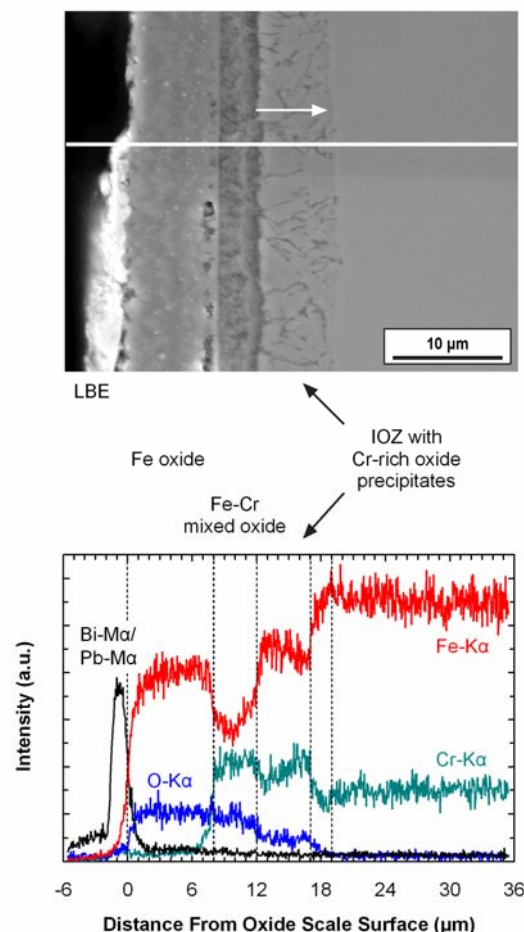
Figure 3 – *Cross-section of T91 after exposure for 1500 h to stagnant, oxygen-saturated LBE at 550°C (specimen J11). Electron-optical micrograph and results of qualitative energy-dispersive X-ray (EDX) micro-analyses.*

material after exposure for 1200 h to flowing LBE in the CORRIDA loop at 550°C and an oxygen content corresponding to a PbO activity, a_{PbO}, between 10^{-4} and 10^{-2}.[1] In the capsule-experiment, a_{PbO} was close to unity (PbO formation on the LBE surface), so that the LBE can be regarded as saturated with oxygen.

The scale found on the surface of specimen J11 (which was prepared for metallographic examination in the state as taken from the capsule) consists of three distinguishable layers (Figure 3). The outermost layer is an Fe-oxide, most likely magnetite, Fe_3O_4. According to findings from a previous study on steels the surface of which was partly alloyed with aluminium (Al) before exposure to oxygen-containing liquid Pb, this layer at the interface with the LBE grows by outward diffusion of Fe.[4] Beneath the Fe-oxide layer, an Fe-Cr mixed-oxide has formed by inward diffusion of oxygen. The mixed oxide is probably a Cr-deficient (Fe,Cr)-spinel, as expressed by the structural formula $Fe(Fe_xCr_{1-x})_2O_4$ with $0<x<1$. The oxygen which passes through the mixed-oxide layer is not completely consumed by the growth of this layer and precipitates as Cr-rich oxide preferentially at grain boundaries within the steel, so that an internal oxidation zone (IOZ) is established. The steel at the IOZ/steel interface may be slightly depleted in Cr, especially in places where a thin, continuous layer of Cr-rich oxide has formed at this interface. However, the thickness of the depleted zone, if present, is in the order of the spatial resolution of energy-dispersive X-ray (EDX) micro-analyses which were performed in order to get semi-quantitative information on the chemical composition of the oxide scale and the steel near the instantaneous steel surface (Figure 3).

3 Pre-exposure measurements

Most of the corrosion processes which occur in a plant or in laboratory experiments cause either an apparent movement of the material surface from the initial position towards the core of the material ("surface recession" or "metal recession" if the material is metallic) or a sub-surface degradation after ingress of a corrosive species into the material. Secondary processes like a corrosion-induced phase transformation in the material can be accompanied by a volume expansion partly compensating the decrease in volume due to material consumption at the surface, while the effect of other secondary processes like corrosion-induced cracking simply adds to the damage caused by the primary corrosion processes. Regardless of the complexity of the underlying corrosion processes, the loss of sound material can always be determined, provided that the part of the material cross-section which still exhibits the desired properties can be unequivocally identified and accurately measured after the corrosive loading, and also provided that the initial geometric dimensions of the material cross-section are known with sufficient accuracy. In special cases, it can be more practical to measure this section loss via the amount of corrosion products formed (i.e., the thickness/mass of a scale of solid corrosion products) on the material surface, which, in general, is only appropriate when (1) sub-surface phenomena do not contribute to the corrosion damage and (2) the physical state of the corrosion products allows for an accurate assessment. In such cases, the knowledge of the initial geometric dimensions would be dispensable. However, as the material behaviour in complex corrosive environments sometimes takes unpredictable turns, an as-accurate-as-practical determination of the initial dimensions is highly recommended, especially for long-term laboratory experiments.

Considering the size of specimens usually employed in laboratory experiments, small changes in geometric dimensions may be measured more precisely using gravimetric methods, i.e., a corresponding area-specific mass change. As mass changes are not sufficiently sensitive to some types of sub-surface degradation, their significance for the loss of sound material must be checked by accompanying metallographic examinations. Additionally, the occurrence of local corrosion phenomena may require a specific analysis of the collected mass change data, when supplemental information from metallographic examinations is not available.[5]

3.1 Initial geometric dimensions

In the case of cylindrical specimens (as those employed in this investigation and also in the exposure experiments in the CORRIDA loop), the diameter is the decisive geometric dimension, the decrease of which in the course of the exposure to oxygen-containing LBE can be used to quantify the progress of material degradation. According to experience from previous exposure experiments in the CORRIDA loop, a determination of the initial diameter using a Vernier calliper or a hand-held micrometer (or a supported micrometer and holding the specimen in hand) is not considered accurate enough, especially after shorter exposure times in the order of 1000 h, for which the expected loss of sound material is around 10 µm (20 µm change in diameter). Therefore, the equipment shown in Figure 5 was set up, which consists of a double-V prism supporting the specimen during the measurement and a displacement transducer with an accuracy of indication of 0.001 mm. The opening angle of the prism is 90° and the tolerances for parallelism and rectangularity, respectively, between horizontal and perpendicular surfaces are both 0.004 mm (manufacturer information). In order to reduce the length of the contact lines between the circular specimen and the V-shaped opening of the prism, and, therefore, minimise the influence of burrs at specimen edges on the measurement, a central gap with a width of 15 mm was cut into the prism (Figure 5 bottom left), resulting in a length of these contact lines of 17.5 mm, which is half the overall length of the specimens. The displacement transducer is equipped with a blade-shaped probe (width: 3.3 mm, thickness: 0.5 mm), so as to ensure that the point of contact with the cylindrical specimen lies on the apex line of the cylinder. The zero-point for the displacement measurement is fixed using a cylindrical calibration piece. For a first series of measurements, a calibration piece with diameter 16.00 mm was used and replaced afterwards with a more precise calibre with diameter 8.002 mm (±0.001 mm).

Figure 6 illustrates the measurements which were performed on the specimens J10 to J14. For each specimen, three cross-sections were measured, one in the centre of the specimen (Section II) and one each in the vicinity of the two ends (Section I and III). For each cross-section, four measurements were performed with the specimen being rotated 90° clockwise after each measurement. J14 was measured four times according to this procedure, two times each using the calibration piece with diameter 16.00 mm and the more accurate one with diameter 8.002 mm, so as to get an idea about the repeatability of the determination of the initial diameter of the specimens, D_0. The results are summarised in Table 1. (J13 and J14 are uncorroded control specimens.)
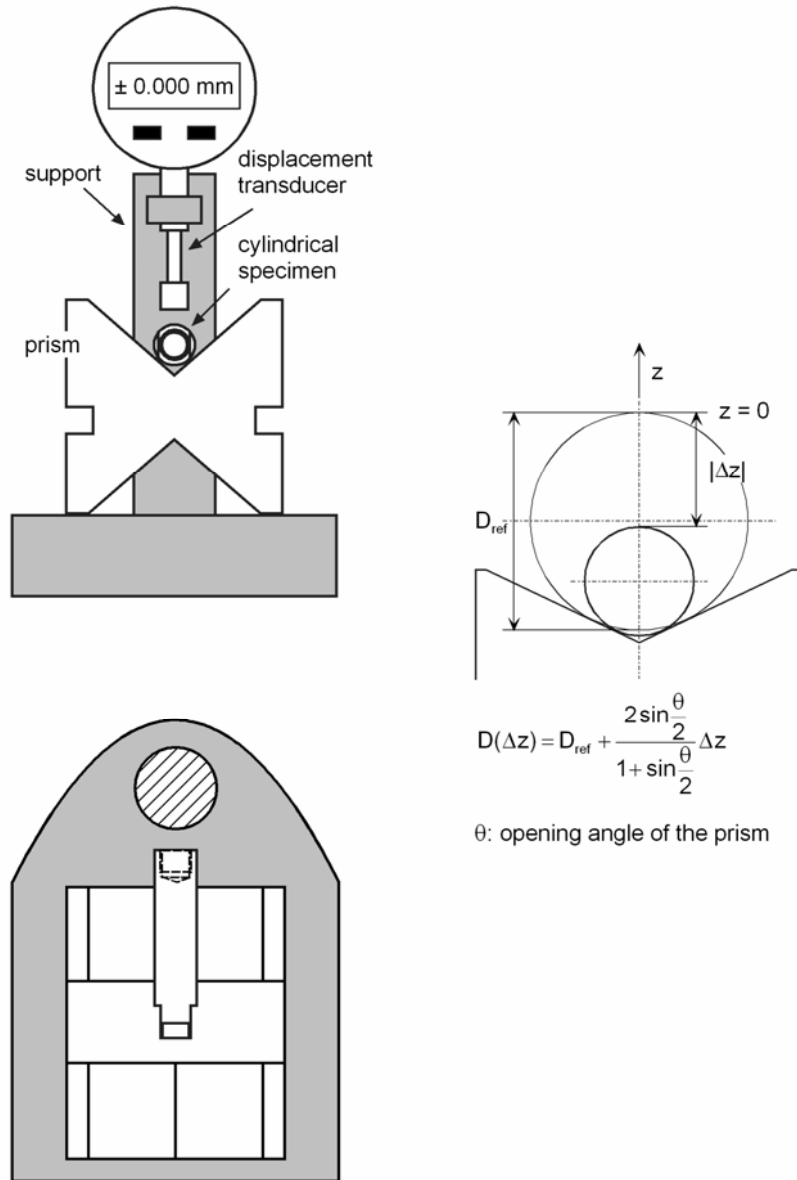
Figure 5 – *Equipment for measuring the initial diameter of cylindrical specimens. D_{ref} is the diameter of a cylindrical calibration piece used to define the zero-point of the displacement Δz, from which the diameter of the specimen is calculated.*
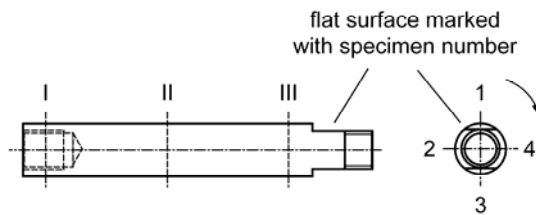
Figure 6 – *Illustration of the measurements performed on each specimen in order to determine the initial diameter and the variation of the diameter along the specimen.*

Table 1 – *Results of the determination of the diameter D_0 on specimens J10 to J14. The diameters were calculated from the measured displacement Δz using the equation given in Figure 5. Bold type: Mean diameter following from the four measurements performed for each cross-section (I to III).*

Specimen	J10	J11	J12	J13	J14			
Diameter of calibration piece (D_{ref} /mm)								
	16.00	16.00	16.00	16.00	16.00	16.00	8.002	8.002
Diameter calculated from measured displacement Δz (D_0 /mm)								
Section I	8.021	8.021	8.023	8.021	8.020	8.018	8.016	8.020
	8.019	8.019	8.021	8.021	8.016	8.015	8.012	8.016
	8.022	8.021	8.022	8.020	8.019	8.018	8.015	8.017
	8.019	8.019	8.021	8.016	8.019	8.017	8.013	8.019
	8.020	**8.020**	**8.022**	**8.020**	**8.018**	**8.017**	**8.014**	**8.018**
Section II	8.021	8.018	8.021	8.019	8.019	8.018	8.014	8.017
	8.019	8.017	8.020	8.019	8.016	8.018	8.014	8.015
	8.020	8.020	8.021	8.018	8.019	8.017	8.014	8.019
	8.019	8.018	8.022	8.020	8.016	8.018	8.014	8.018
	8.020	**8.018**	**8.021**	**8.019**	**8.017**	**8.018**	**8.014**	**8.017**
Section III	8.028	8.027	8.033	8.026	8.026	8.025	8.022	8.025
	8.023	8.026	8.032	8.028	8.021	8.023	8.019	8.020
	8.026	8.026	8.029	8.023	8.022	8.023	8.019	8.022
	8.026	8.026	8.035	8.026	8.025	8.025	8.020	8.026
	8.026	**8.026**	**8.032**	**8.026**	**8.023**	**8.024**	**8.020**	**8.023**

Considering only the measurements performed on Sections I and II of each specimen, the variation between the four diameters determined for the same cross-section mostly is ≤ 3 µm, resulting in a deviation of the single values from the calculated mean diameter ≤ 2 µm (Table 1). The deviation of the mean diameter determined for Section I from that of Section II within the same series of measurements is also ≤ 2 µm. Looking at the results of the repeated measuring of J14, the variation in the determined mean values is 1 µm for the two series of measurements in which the calibration piece with diameter 16.00 mm was used to define the zero-point for the displacement Δz, and 3-4 µm for the two series of measurements in which the more precise calibre with diameter 8.002 mm was used. The measurements performed on Section III of each specimen exhibit more significant variations in the results of the single measurements on the same cross-section and also a comparatively large deviation of the mean value from the mean diameter determined for Sections I and II of the same specimen. This discrepancy most likely results from the edges (parallel to the long axis of the cylindrical specimen) which originated from machining the flat surfaces at the specimen end with the external screw-thread (see Figure 1). These edges, on which a tiny burr may have formed during the surface-finish of the specimens, rested in the V-shaped opening of the prism when Section III was measured. For measurements on Sections I and II of the specimens, the repeatability of the diameter measurement is probably better than 4 µm, with variations of around 2 µm being possibly due to the surface roughness of the specimens.

Table 2 – *Results of control measurements on the calibration pieces. The three cross-sections measured in each series were uniformly distributed along the length (70 mm) of the calibration pieces.*

Measured calibration piece	8.002	16.00	
D_{ref} /mm	8.002	8.002	8.002
First section	8.002	15.999	15.999
	8.001	15.999	15.999
D/mm	8.004	15.999	15.999
	8.005	15.998	15.999
	8.003	**15.999**	**15.999**
Second section	8.002	15.995	15.997
	8.000	15.995	15.996
D/mm	8.004	15.995	15.996
	8.003	15.995	15.997
	8.002	**15.995**	**15.997**
Third section	8.002	15.996	16.000
	8.004	15.995	16.000
D/mm	8.005	15.996	16.000
	8.005	15.997	16.000
	8.004	**15.996**	**16.000**

Finally, additional measurements on the calibration pieces were performed, in order to get more information on the accuracy of the prism method and also to prove the precision of the calibre with diameter 16.00 mm. Three cross-sections were measured in each series, with the series of measurements on the calibre with diameter 16.00 mm repeated once. Considering that the calibration piece with diameter 8.002 has a manufacturing tolerance of ± 1 µm, the measurements with the introduced equipment are accurate within 2 to 4 µm (Table 2), which compares well with the repeatability of the measurements on the specimens. The diameter of the calibration piece with nominal 16.00 mm is 16.000 (-0.005) mm.

3.2 Initial mass

The initial mass of the specimens J10, J11 and J12 was determined using a laboratory balance (Sartorius BP211D) with an accuracy of indication of 0.00001 g (0.01 mg), which is in accordance with guidelines for corrosion testing.[3] Each specimen was weighed three times, and the mean value was taken as the initial mass, m_0 (Table 3). The repeatability of the measurements is between ± 0.01 and ± 0.04 mg, which also compares fairly well with recommendations for corrosion testing (± 0.02 mg).[3] The surface area exposed to LBE in the course of the experiment is specified as 7.791 cm² for the specimens employed in this investigation, corresponding to the size of the curved surface of a cylinder with diameter 8 mm and length 31 mm. The flattened part of the surface near the specimen end with the external screw-thread was neglected in the calculation of the exposed surface (see Figure 1).

Table 3 – *Initial mass, m_0, of specimens J10, J11 and J12. The surface area exposed to LBE in the experiments is 7.791 cm².*

	First measurement	Second measurement	Third measurement	**m_0 (g)**
J10	10.27937	10.27939	10.27938	10.27938
J11	10.27437	10.27442	10.27437	10.27438
J12	10.28741	10.28744	10.28745	10.28743

4 Post-exposure measurements

The main objective of post-exposure measurements is to deliver quantitative information on the part of the initial material cross-section which still exhibits the desired (mechanical) properties. There is a choice of methods for measuring this part of the cross-section either directly or indirectly (e.g., via the dimensions of an adherent scale of corrosion products), the appropriateness of which strongly depends on the type of corrosion damage occurring in the regarded case. As the dissolution of material constituents (Fe) and, when considering the lower temperatures in a non-isothermal apparatus, also their re-precipitation (in the form of oxides) can be important for the behaviour of steels in oxygen-containing LBE, direct measurements of the remaining cross-section should be preferred. If the dimensions and composition of the adherent oxide scale are determined in addition to the dimensions of the remaining cross-section of the steel, the amount of metal transferred between the solid phases (steel and adherent oxide scale) and the LBE can be estimated, which provides valuable supplemental information for mechanistic considerations. However, transfer of steel constituents between the solid phases and the LBE is possible not only due to dissolution and re-precipitation, but may also result from erosion or partial spalling of the oxide scale, especially in the case of flowing LBE.

Two methods for determining the dimensions of the remaining cross-section and the adherent oxides are introduced, the first of which is based on measurements under a light-microscope on specimens prepared using metallographic techniques (metallographic method). The second (gravimetric) method is based on weighing corroded specimens with and after removal of adherent oxides. The latter method necessitates stripping remnants of LBE (adhering to the specimen after the exposure to the corrosive environment) off the oxide-scale surface without removing significant amounts of oxide. In a next step, the oxide scale—in the case of T91, the magnetite and spinel layer and the internal oxidation zone (IOZ)—has to be removed without loss of underlying steel.

4.1 Successive removal of adherent LBE and oxide scale

An especially gentle method of stripping LBE from the surface of an oxide scale is to dip the oxidised specimen repeatedly into hot vegetable fat (160°-180°C) and dabbing carefully at the surface with a piece of cloth, so as to swab remnants of molten LBE away. This procedure was successfully applied in preparing oxidised
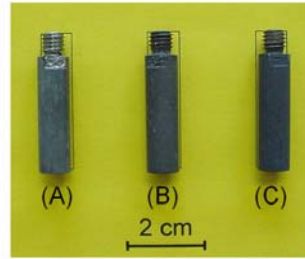
(A) as taken from the oxidising LBE
(B) after treatment with hot fat
(C) after additional treatment with half-concentrated nitric acid

Figure 7 – Specimens of T91 after exposure for 1500 h to stagnant oxidising LBE at 550°C and different stages of the removal of adherent LBE. (A): Specimen J11 as taken from the oxidising LBE. (B): Specimen J12 after treatment with hot fat. (C): Specimen J10 after additional treatment with half-concentrated nitric acid.

specimens for recording X-ray-diffraction (XRD) spectra from the oxide-scale surface, amongst others, by the colleagues from the Institute for Pulsed Power and Microwave Technology, Forschungszentrum Karlsruhe. For treating the cylindrical specimens of (magnetic) T91, the procedure was slightly modified, i.e., a heating plate with an integrated magnetic stirring device was used, so as to rotate the specimen in the hot fat, which due to centrifugal forces more efficiently removes the molten LBE from the surface and from inside the internal screw-thread at one end of the specimen. After air-cooling, the specimen surface exhibits a greyish hue, indicating a thin film or stains of LBE left on the surface that would not seriously disturb the XRD analysis, but, owing to the comparatively high density of LBE, can cause a significant error in the oxide mass. These minor remnants of LBE are removed by treating the specimen for about 5 min with a 1:1 mixture of concentrated nitric acid (65 mass-% HNO_3) and water in an ultrasonic bath. After subsequent rinsing with deionised water and drying in air, the oxide-scale surface appears black without a greyish tint. Some oxide particles (magnetite) detach from the oxide scale during the treatment with nitric acid most likely from to the simultaneous application of ultrasound. A photograph of specimens after different stages of the removal of adherent LBE is shown in Figure 7.

For removing the oxide scale from the surface of T91, two methods were examined, which were successfully applied by the authors in other cases of corrosion. The first of these methods, i.e., stripping with molten sodium hydroxide (NaOH) at 400°C was tested for 15 min on specimen J10 after removal of adherent LBE. There was hardly any effect on the oxide scale on T91, so that the treatment with molten NaOH was not followed up. The second method is based on the alternate treatment with boiling alkaline potassium permanganate ($KMnO_4$) solution and inhibited hydrochloric acid ($HCl_{inhib.}$). The treatment with $HCl_{inhib.}$, which also removes a thin tarnish film that forms on the steel in the $KMnO_4$ solution, is performed in an ultrasonic bath at room-temperature. After each step of the pickling procedure, the specimens are rinsed with deionised water. The composition of the solutions is listed in Table 4.

Table 4 *– Composition of pickling solutions and further details on the application to oxidised T91.*

	alkaline potassium permanganate solution	**inhibited hydrochloric acid**
composition	900 ml water 28.8 g potassium permanganate 90 g sodium hydroxide	833 ml water 167 ml hydrochloric acid (37 mass-% HCl) 2 g hexamethylene tetramine ($(CH_2)_6N_4$)
temperature	boiling (~100°C)	room-temperature
ultrasound	no	yes

The alternate treatment with alkaline $KMnO_4$ solution and $HCl_{inhib.}$ was tested on specimens J10 and J12 (after stripping the LBE). The two solutions were repeatedly applied, with the duration of treatment with $HCl_{inhib.}$ varied. As a basis for judging on the efficiency with respect to the removal of the oxide layers and stripping the IOZ, the specimens were weighed and optically inspected between the single steps of the pickling procedures. After the last step, metallographic cross-sections of the specimens were prepared for microscopic investigation, so as to check for remnants of the IOZ. The pickling procedures as applied to J10 and J12 are summarised in Table 5.

Figure 8 shows micrographs of the cross-section of specimens J10 and J12, respectively, after the alternate treatment with boiling alkaline $KMnO_4$ solution and $HCl_{inhib.}$. Such a treatment is capable of stripping the oxide layers (magnetite, spinel) and the IOZ from the steel surface, with the procedure applied to J10 being some-what more efficient. J12 still exhibits remnants of the IOZ (dark-grey stains on the otherwise matt, steel-grey surface), while, in the case of J10, such remnants of the IOZ are the exception. The striking difference between the two pickling procedures is that J10 was treated for about 1 h with $HCl_{inhib.}$ after the first treatment with alkaline $KMnO_4$ solution, which seems to be necessary to degrade the IOZ and makes the IOZ susceptible for detachment. The simultaneous application of ultrasound probably promotes this process. The alternate treatment with the $KMnO_4$ solution for 30 min and $HCl_{inhib.}$ for 5 min as applied to J12 is less efficient.

Table 5 *– Summary of the pickling procedures applied to specimens J10 and J12 in order to remove the adherent oxide scale.*

J10	**J12**
Pickling procedure:	
1) boiling alkaline $KMnO_4$ for 30' 2 a) inhibited hydrochloric acid for 5' 2 b) inhibited hydrochloric acid for 1 h	1.) boiling alkaline $KMnO_4$ for 30' 2.) inhibited hydrochloric acid for 5'
3.) boiling alkaline $KMnO_4$ for 30' 4.) inhibited hydrochloric acid for 10'	3.) boiling alkaline $KMnO_4$ for 30' 4.) inhibited hydrochloric acid for 5' 5.) boiling alkaline $KMnO_4$ for 30' 6.) inhibited hydrochloric acid for 5'
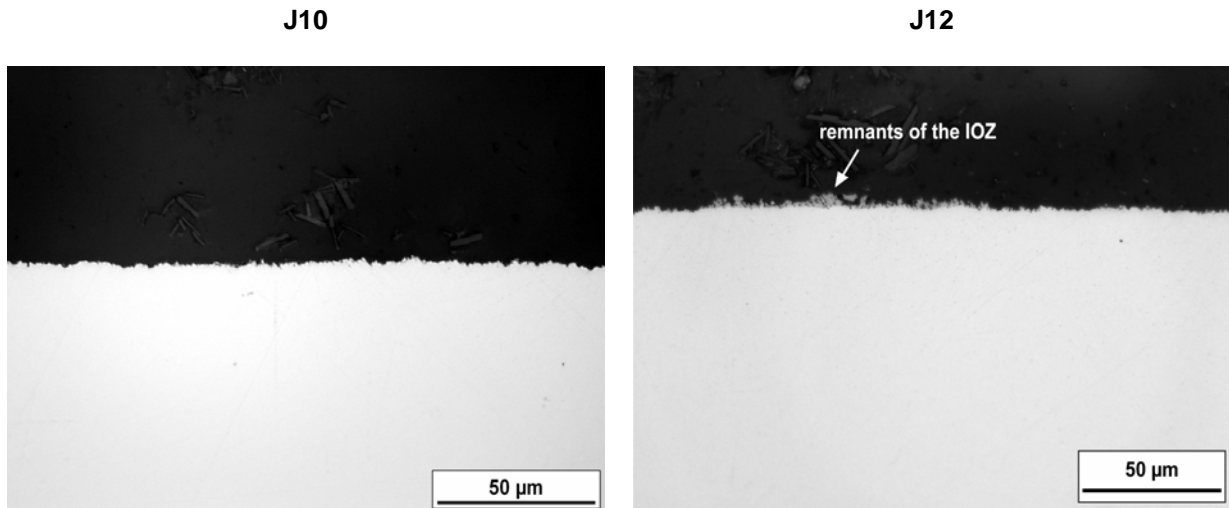
Figure 8 – Light-optical micrographs of the cross-section of specimens J10 (left) and J12 after pickling. Specimen J12 exhibits considerable amounts of remnants of the IOZ, the thickness of which can be locally up to 7 µm.

4.2 Metallographic method

4.2.1 Description of the method

For measuring the diameter of metal with sound properties after the corrosive loading and the thickness of distinguishable parts of the oxide scale under the light-microscope, an approximately 5 mm thick slice is cut from the specimen and pre-pared using standard metallographic techniques. The final polishing is performed with 1 µm diamond suspension. The microscope employed in this investigation is a binocular Leitz Ergolux AMC, the stage of which can be shifted in the x- and y-directions with an accuracy of 1 µm via a control device connected to the microscope (Leitz LAF AMF/Scan 2000). One of the oculars contains crosshairs which are used as a marker for positioning the specimen via the movable microscope stage. The measurements are performed at 500-fold magnification.

The measurement starts with positioning the specimen so that one of the crosshairs forms a tangent at the IOZ/steel interface, which is regarded as the boundary of the metal with sound properties (dashed crosshairs in Figure 9). This position is defined as the zero-point. Subsequently, the microscope stage is moved via the control device, until the same hair forms a tangent at the IOZ/steel interface on the opposite side of the cross-section. The diameter of sound metal can then be calculated from the shift of the microscope stage in the planar directions, X_1 and X_2, according to Figure 9, with X_1 being defined as the larger shift for each measure-ment. The smaller shift X_2 arises from differences in orientation between the cross-hairs and the x- and y-directions of the microscope stage, but can also indicate that the tangential positions have not exactly been matched. However, if the crosshairs have been fairly well aligned with the moving directions of the microscope stage, the influence of X_2 on the calculated diameter is negligible. The diameter of sound metal is measured six times, with the first measurement being performed for an arbitrarily

$$D=\sqrt{X_1^2 + X_2^2}$$
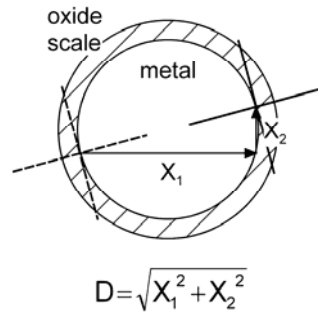
Figure 9 – *Determination of the diameter of sound metal under the light-microscope.*

chosen orientation of the specimen in relation to the crosshairs (and moving directions of the microscope stage). When vertical crosshair has been used in the first measurement, the second measurement is performed using the horizontal crosshair and *vice versa*. Afterwards, the specimen is rotated by hand approximately 30°, and the third and fourth measurement are performed using the same crosshair as in the second and first measurement, respectively. The fifth and sixth measurement are performed analogously after another 30° rotation of the specimen, so that the first and second, third and fourth, fifth and sixth diameter are each pairs of orthogonal diameters, which, as discussed below, can be important when interpreting the results. The thickness of the distinguishable parts of the oxide scale (magnetite, spinel, IOZ) is determined twelve times, again using the crosshairs as a marker for positioning the specimen and measuring in pairs as described above. If a near-surface zone in which the steel is depleted in one or more constituents (e.g., Cr) has to be considered, etching of the cross-section may be necessary to determine the part of the cross-section with sound properties and the thickness of the depleted zone. In this case, the oxide scale should be measured before etching. In the presented investigation, a depleted zone was not considered.

4.2.2 Measurements

The described method was applied in full to specimen J11 which was prepared for examination under the microscope in the as-received state after exposure to oxidising LBE. The investigated cross-section coincides approximately with Section II of the pre-exposure measurement of the diameter (see Figure 6). Specimens J10 and J12 were measured after removal of adherent LBE and the oxide scale so that only the diameter of sound metal was determined. In the case of J10, two sections of the specimen were examined, which approximately coincide with Section I and Section II in Figure 6. In the case of J12 only one section approximately coinciding with Section II of the pre-exposure measurement was examined. The results are summarised in Table 6.

In order to prove the reliability of the diameter measurements under the microscope, the diameter of the uncorroded control specimens J13 and J14 was remeasured using to the metallographic method in a position along the specimen which approximately coincides with Section II in Figure 6. The measurement on J13 was repeated once. The results are listed in Table 7.

Table 6 – *Results of post-exposure measurements under the microscope. D_1 is the measured diameter of sound metal. δ_{Mag}, δ_{Spi}, δ_{IOZ} and δ denote the thickness of the magnetite and spinel layers, the internal oxidation zone and the overall scale thickness, respectively. The position of Section I and Section II along the specimen follows from Figure 6. The minima of the diameter measurements are underlined.*

	J10 Section I D_1 (mm)	J10 Section II D_1 (mm)	J11 Section II D_1 (mm)	δ_{Mag} (µm)	δ_{Spi} (µm)	δ_{IOZ} (µm)	δ (µm)	J12 Section II D_1 (mm)
	8.037	<u>8.002</u>	8.004	9	5	5	19	8.000
				9	3	6	18	
	<u>8.004</u>	8.015	7.998	6	3	5	14	7.998
				14	5	7	26	
	8.005	8.017	8.001	10	5	6	21	7.996
				9	2	8	19	
	8.029	8.005	8.000	11	6	6	23	8.000
				7	3	8	18	
	8.014	8.015	<u>7.993</u>	7	2	7	16	8.006
				13	6	8	27	
	8.017	8.016	8.008	8	3	6	17	<u>7.995</u>
				9	4	8	21	
Mean value	8.018	8.012	8.001	9	4	7	20	7.999
Standard deviation	0.0131	0.0063	0.0051	2.4	1.4	1.2	3.9	0.0040

Table 7 – *Results of re-measuring the diameter of specimens J13 and J14 according to the metallographic method. D_m and s denote the mean value and the standard deviation of the diameter measurements.*

	D/mm						D_m /mm	s/mm
J13 Section II	8.018	8.022	8.017	8.016	8.017	8.016	8.018	0.0022
Repetition	8.017	8.016	8.016	8.017	8.020	8.021	8.018	0.0021
J14 Section II	8.016	8.025	8.028	8.017	8.018	8.021	8.021	0.0048

14

Comparing the diameters for J13 from the measurements under the microscope with the results of the prism method for measuring the initial diameter, D_0, before the exposure experiment, there is a good correspondence between the two techniques (Table 7 and Table 1, J13 Section II). The calculated mean diameters differ by only 1 µm and also the deviation of single measurements from the mean is comparable (2-4 µm in comparison to 2 µm for the pre-exposure measurements). Looking at the results for J14, the difference between the mean diameter following from the measurements under the microscope and the mean value obtained for D_0 (Table 1, J14 Section II) is in the range of 5 µm, and especially the deviations between the single diameter measurements according to the metallographic method are considerably larger than in the case of J13 (Table 7). These larger deviations in the single values can be explained, when considering the pairs of orthogonal diameters resulting from the measurements under the microscope (which are separated from each other by dashed lines in Tables 6 and 7). Such a pair consists of either a small and a large diameter or two intermediate diameters, indicating an elliptical distortion of the examined cross-section. This distortion of an originally circular section, which can especially be seen in the results of the diameter measurements on Section I of J10 (Table 6), can arise when the cylindrical specimen was not exactly cut perpendicular to the long axis or from a tilt of the metallographically mounted piece of the specimen with respect to the plane of the grinding wheel during preparation for microscopic examination. In this case, the minimum diameter measured under the microscope is the best estimate for the true diameter of the circular cross-section. The deviation of the minimum diameter measured on the cross-section of J14 under the microscope from the mean value obtained for D_0 is in the range of 1-2 µm.

The effect of a slight elliptical distortion of the prepared cross-section on the measured thickness of the distinguishable parts of the oxide scale is negligible in comparison with the limited accuracy of the thickness measurements (1 µm).

4.3 Gravimetric method

For the determination of the mass of the oxide scale and the change in the mass of sound metal, the specimens J10 and J12 were re-weighed after stripping the LBE (m_1) and after subsequent removal of the oxide scale (including the IOZ, m_2). Three measurements each were performed, the results of which are listed in Table 8 together with the respective mean values. In the case of J12, the final step in the procedure of stripping the LBE (treatment with nitric acid) was not performed and, as discussed in subsection 4.1 of this report, remnants of the IOZ after removal of the oxide scale may have caused a considerable error in the mass m_2. Therefore, the respective masses are denoted $m_1{}^*$ and $m_2{}^*$ in Table 8.

Looking at the results of the single measurements of m_1 for specimen J10 and $m_2{}^*$ for J12, there is a significant scatter in the obtained data. This scatter is possibly due to loosely adherent oxide particles or moisture (from imperfect drying after the treatment with diverse aqueous solutions) on the rough and porous specimen surface. However, in view of the differences between the measured values of m_1 and m_2 and the respective initial mass m_0 (Table 3), it can be expected that the resulting inaccuracy of calculated mass changes is in the range of 1-10%, which should be still sufficiently accurate to evaluate the gravimetric versus the metallographic method.

Table 8 – *Results of re-weighing specimens J10 and J12 after stripping the LBE (m_1) and after subsequent removal of the oxide scale (m_2). In the case of J12, the final step in the procedure of stripping the LBE (treatment with nitric acid) was not performed (error in m_1) and, furthermore, remnants of the IOZ after removal of the oxide scale may have caused a considerable error in the mass m_2. Therefore, the respective masses are denoted m_1* and m_2*.*

		First measurement	Second measurement	Third measurement	**Mean value**
J10	**m_1 (g)**	10.30740	10.30713	10.30725	10.30726
	m_2 (g)	10.20562	10.20568	10.20563	10.20564
J12	**m_1* (g)**	10.34971	10.34970	10.34974	10.34972
	m_2* (g)	10.24471	10.24419	10.24462	10.24451

5 Evaluation and discussion of the results

5.1 Metal recession

The diameters of sound metal after the exposure to oxidising LBE, which were measured on specimens J10, J11 and J12 according to the metallographic method (Table 6), and the respective initial diameters, D_0 (Table 1), were used to calculate the change in the diameter of sound metal, ΔD. The results are listed in Table 9. In order to account for a potential elliptical distortion of the cross-sections during the preparation for microscopic examination, both the mean, $D_{1(mean)}$, and minimum value, $D_{1(min)}$, of the measurements under the microscope were considered. The results for J10, both in Section I and Section II, clearly indicate such a distortion of the examined cross-section, so that $D_{1(min)}$ is probably a better estimation of the true (mean) diameter of sound metal after the exposure than $D_{1(mean)}$. In the case of the other specimens, it is not clear, whether the mean or the minimum of the measured

Table 9 – *Change in the diameter, ΔD, and radius of sound metal, ΔR, calculated from the initial diameter, D_0, and the diameter of sound metal after exposure for 1500 h to stagnant, oxygen-saturated LBE at 550°C, D_1. D_1 was determined according to the metallographic method, where the subscript (mean) and (minimum) denote that the mean and minimum value of the measurements under the microscope were used for the calculations.*

		D_0 (mm)	$D_{1(mean)}$ (mm)	$\Delta D_{(mean)}$ (mm)	$\Delta R_{(mean)}$ (mm)	$D_{1(min)}$ (mm)	$\Delta D_{(min)}$ (mm)	$\Delta R_{(min)}$ (mm)
J10	**Section I**	8.020	8.018	(− 0.002)	(− 0.001)	8.004	− 0.016	− 0.008
	Section II	8.020	8.012	(− 0.008)	(− 0.004)	8.002	− 0.018	− 0.009
J11	**Section II**	8.018	8.001	− 0.017	− 0.009	7.993	− 0.025	− 0.013
J12	**Section II**	8.021	7.999	− 0.022	− 0.011	7.995	− 0.026	− 0.013

Table 10 – *Mass change of sound metal, Δm_M, and corresponding metal recession, $|\Delta R|$, for T91 after exposure for 1500 h to stagnant, oxygen-saturated LBE at 550°C calculated from the initial mass, m_0, and the mass after exposure and subsequent removal of the oxide scale, m_2.*

	m_0 /g	m_2 /g	Δm_M /g	$|\Delta R|$/μm
J10	10.27938	10.20564	– 0.07374	12
J12	10.28743	10.24451	– 0.04292	7

diameters is more reliable, since the deviation of the calculated changes in diameter are in a range which could result from the measuring error of the applied method or non-uniformity of the corrosive attack along the specimen circumference.

The loss of sound material (metal recession) due to oxidation is the absolute amount of the change in radius, ΔR. According to Table 9, the metal recession, $|\Delta R|$, of T91 under the experimental conditions (stagnant, oxygen-saturated LBE/550°C/ 1500 h) is in the range of 8-13 μm.

Alternatively, $|\Delta R|$ can be calculated from the mass after exposure and removal of adherent oxides (including the internal oxidation zone, IOZ), m_2, and the initial mass before the exposure, m_0. The difference ($m_2 - m_0$) is the mass change of sound metal, Δm_M, the absolute amount of which has to be divided by the exposed surface area, A, and the density of the steel, ρ_{steel}, i.e.,

$$|\Delta R| = \frac{|\Delta m_M|}{A\,\rho_{steel}}$$

(1)

For the specimens employed in this investigation, the exposed surface area is A = 7.791 cm². The density of T91 is ρ_{steel} = 7.7 g/cm³.

The results of calculating Δm_M and $|\Delta R|$ using the values for m_2 in Table 8 and m_0 according to Table 3 are listed in Table 10. In the case of specimen J10, $|\Delta R|$ from the gravimetric method (12 μm) compares well with the range for $|\Delta R|$ obtained by the measurements under the microscope (8-13 μm, Table 9). This good correspondence can be regarded as a confirmation of the somewhat ambiguous results of the metallographic method, and additionally shows that the procedure of removing the oxide scale chosen for J10 is appropriate for a quantitative analysis of the metal loss due to oxidation (at least within the range of error of the metallographic method). In the case of J12, the gravimetric method yields a significantly smaller $|\Delta R|$, which is out of the range determined using the metallographic method because of the imperfect removal of the IOZ with the pickling procedure chosen for J12 (see Section 4.1 of this report).

5.2 Oxide scale thickness and metal dissolution

Another important point to be clarified is how the dimensions, i.e., thickness or mass, of the oxide scale relate to the metal recession and if conclusions on the amount of constituents of the steel transferred between the solid phases (steel and

adherent oxide scale) and the LBE can be drawn. Metal dissolution (after diffusion through the oxide scale or reduction of oxide at the scale surface) is one possible mechanism for such a mass transfer, but, alternatively, parts of the oxide scale can spall off or may be eroded in the case of flowing LBE. These processes can probably be distinguished from metal dissolution on the basis of the surface profile of the oxide scale, with a pronouncedly irregular surface profile indicating spalling or erosion. Considering the lower temperatures in a non-isothermal apparatus, metals that stem from the LBE can be incorporated into the oxide scale, e.g., through re-precipitation of dissolved steel constituents in the form of oxides.

Provided that the composition and thickness of the adherent oxide scale and the metal recession are known, criteria for the transfer of steel constituents between the solid phases and the LBE can be established on the basis of the Pilling-Bedworth ratio. The Pilling-Bedworth ratio, Φ, is defined as the volume of solid oxide formed from 1 mol metal divided by the molar volume of the metal, and, for exclusive formation of M_3O_4 type oxides (magnetite, spinel) on ferritic Fe-Cr alloys, it is slightly larger than 2 ($\Phi \approx 2.1$-2.2), which is also assumed to be valid for the formation of these oxides on martensitic steels like T91. This means that the thickness, δ, of an oxide scale on the surface of T91 consisting exclusively of M_3O_4 type oxides should be approximately twice the metal recession, $|\Delta R|$. Accordingly, if the constituents of the steel were partly transferred to the corrosive environment then $\delta < 2\,|\Delta R|$, or if the metal incorporated into the scale partly stems from the environment then $\delta >> 2\,|\Delta R|$. However, the scale observed on T91 after exposure to oxygen-containing LBE does not exclusively consist of layers of M_3O_4 type oxides, but also exhibits an IOZ of considerable thickness (Figure 3). The IOZ can be regarded as a heterogeneous layer of the oxide scale, containing an oxide phase richer in Cr than the Cr-deficient spinel on top of the IOZ (e.g., stoichiometric spinel or a Cr-rich α-M_2O_3) and a metallic phase (Cr-depleted steel) the density of which is significantly higher than the density of oxides. Accordingly, if considering the IOZ as part of the oxide scale ($\delta = \delta_{(+IOZ)}$), $\delta_{(+IOZ)}$ can be $< 2\,|\Delta R|$ without necessarily involving transfer of metal to the LBE. In the case that the IOZ is not counted in both the oxide scale thickness ($\delta = \delta_{(-IOZ)}$) and metal recession ($|\Delta R| = |\Delta R|_{(-IOZ)}$), a significant positive deviation of $\delta_{(-IOZ)}$ from $2\,|\Delta R|_{(-IOZ)}$ does not necessarily mean that metal stemming from the LBE has been incorporated into the scale, as the volume balance in the IOZ requires that a part of the metal contained in the steel volume consumed by the growth of the IOZ must leave the IOZ and may be bound in the magnetite and/or spinel layer. Thus, even qualitative information on metal transfer cannot be retrieved from the thickness of the oxide scale and the metal recession without additional information on the composition of the IOZ (volume fraction, type and Fe:Cr ratio of the oxide). Determining the composition of the IOZ requires an examination with especially space- and composition-sensitive micro-analysis techniques, e.g., Auger-Electron-Spectroscopy (AES). If a depletion (Cr-depleted) zone is established beneath the IOZ, the composition of this zone must also be considered in a quantitative analysis of metal transfer.

In the case of transfer of steel constituents from the solid phases to the LBE (e.g., metal dissolution), another criterion can be established, which is based on the direction of growth of the spinel and magnetite layers. According to the findings from martensitic steel the surface of which was partly alloyed with Al before exposure to oxygen-containing liquid Pb at 550°C (no remarkable oxidation on the surface-alloyed part), the spinel/magnetite interface approximately coincides with the initial

position of the steel surface.[4] That the spinel and magnetite layers predominantly grow inward and outward, respectively, was also the impression from the post-test analysis of T91 after exposure to flowing, oxygen-containing LBE at 550°C[1] and was stated by other authors as one possible scenario for the oxidation in liquid Pb-alloys.[6] In this particular case, $\Phi \approx 2$ for the formation of M_3O_4 type oxides on ferritic or martensitic steels implies that the thickness of the outward-growing magnetite layer, δ_{Mag}, approximately equals the thickness of the inward-growing spinel layer, δ_{Spi}, if the effect of internal oxidation and depletion of certain constituents in the steel is negligible and transfer of metal to the LBE does not occur. Allowing for internal oxidation yields $\delta_{Mag} > \delta_{Spi}$ in the absence of metal transfer to the LBE, when the, in comparison to Cr, chemically more-noble Fe leaves the IOZ and, after diffusion through the scale, participates in the growth of magnetite on the surface of the magnetite layer. Thus, $\delta_{Mag} < \delta_{Spi}$ is a necessary criterion for a transfer of metal from the solid phases to the LBE in the presence of internal oxidation, that can easily be proved using only the results of the measurements under the light-microscope. Furthermore, $(\delta_{Spi} - \delta_{Mag})$ allows for estimating the amount of metal (predominantly Fe) transferred to the LBE, with this estimation being more accurate the less important the influence of internal oxidation. Looking at the results for the thickness of the distinguishable parts of the oxide scale on T91 after exposure to stagnant, oxygen-saturated LBE at 550°C (Table 6, J11), the relationship between the thickness of the magnetite and spinel layer is always $\delta_{Mag} > \delta_{Spi}$, and, accordingly, a significant transfer of metal to the LBE (dissolution of Fe) is unlikely. In flowing LBE at 550°C and $10^{-4} < a_{PbO} < 10^{-2}$, $\delta_M \approx \frac{1}{2}\delta_S$ for the oxide scale on T91 (after exposure for 1200 h),[1] which, following the argumentation above, clearly indicates transfer of metal to the LBE. Neglecting the influence of the IOZ, approximately half the thickness of the magnetite layer is missing, whereby the amount of metal (Fe) transferred to the LBE corresponds to the Fe-content of the missing part of the magnetite layer.

The approximate correspondence of the magnetite/spinel interface with the initial position of the steel surface also implies that the sum of the thicknesses of the spinel layer, δ_{Spi}, and the IOZ, δ_{IOZ}, approximates the metal recession, $|\Delta R|$, which can be used to prove this crucial assumption. Calculating $(\delta_{Spi} + \delta_{IOZ})$ from the values measured on specimen J11 (Table 6) yields a metal recession between 8 and 14 µm with an arithmetic mean of 11 µm, which compares well with the results for $|\Delta R|$ obtained from the metallographic method (8-13 µm) and gravimetric measurement (12 µm). This finding substantiates the correspondence of the magnetite/spinel interface with the initial position of the steel surface and corroborates the introduced method of estimating the amount of metal transferred to the LBE. Additionally, determining $|\Delta R|$ from δ_{Spi} and δ_{IOZ} is also a method of quantifying the metal recession for those combinations of steel and corrosive medium which are known for fulfilling the underlying assumptions. According to the authors' experience with the behaviour of steels in oxygen-containing LBE, some martensitic steels with 9-12 mass-% Cr fulfil this pre-requisite for up to 10,000 h of exposure to oxygen-containing LBE, while for austenitic steels this still has to be proven. As both the metallographic and gravimetric method of quantifying the metal recession tend to be less accurate for shorter exposure times (elliptical distortion during metallographic preparation, remnants of scale after removal of oxides, etc.), quantifying the metal recession on the basis of the thickness of distinguishable parts of the oxide scale is possibly the most accurate of the three methods introduced in this report when considering short-term

19

exposures. However, this method loses its applicability when partial spalling of the spinel layer occurs.

The gravimetric measurements provide an alternative means of determining the oxide scale thickness and quantifying the transfer of steel constituents between the solid phases and LBE. The mass of the scale, m_{scale}, equals $(m_1 - m_2)$, with m_1 being the mass of the steel specimen after exposure to the corrosive environment and stripping of adherent LBE; m_2 is the specimen mass after subsequent removal of the oxide scale including the IOZ. The thickness of the oxide scale, δ, follows as

$$\delta = \frac{m_{scale}}{A \rho_{scale}} \tag{2}$$

where A and ρ_{scale} denote the exposed surface area (A = 7.791 cm² for the specimens employed in this investigation) and the mean density of the oxide scale, respectively. Owing to the lack of information on the composition of the IOZ (volume fraction, type and composition of the precipitated oxides), only the magnetite and spinel layer are considered in the mean density of the scale ($\rho_{scale} \approx 5$ g/cm³), which underestimates the actual mean density of the scale and explains why the larger values for δ from the single measurements under the microscope (Table 6) correspond better to the gravimetric results (Table 11) than the mean value for δ from the metallographic method. In view of the considerable inaccuracy in the masses m_1 and m_2 of specimen J12 argued in Section 4.3 of this report, the δ obtained for J12 coincides surprisingly well with the δ for specimen J10, indicating that the errors in m_1 and m_2 tend to cancel each other in the difference $(m_1 - m_2)$.

The quantitative information on the metal transfer between the solid phases and the LBE follows from comparing the mass of steel constituents (Fe, Cr) in the scale, $m_{M(scale)}$, and the mass change of sound steel, Δm_M. $m_{M(scale)}$ is given by

$$m_{M(scale)} = w_{M(scale)} \, m_{scale} \tag{3}$$

where $w_{M(scale)}$ denotes the mean mass fraction of metals in the scale. For exclusive formation of M_3O_4 type oxides, $w_{M(scale)}$ is

$$w_{M(scale)} = \frac{3M_M}{3M_M + 4M_O} \tag{4}$$

Table 11 – Thickness, δ, and mass of metal, $m_{M(scale)}$, in the oxide scale on T91 after exposure for 1500 h to stagnant, oxygen-saturated LBE at 550°C calculated from the mass after exposure and stripping of LBE, m_1, and the mass after additional removal of the oxide scale, m_2.

	m_1 /g	m_2 /g	$(m_{scale} = m_1 - m_2)$ /g	δ /µm	$m_{M(scale)}$ /g
J10	10.30726	10.20564	0.10162	26	0.0735
J12	10.34972	10.24451	0.10521	27	0.0761

where M_M and M_O are the mean molar weight of metals in the scale and the molar weight of oxygen ($M_O = 16$ g/mol), respectively. When assuming that M_M approximately coincides with the molar weight of Fe ($M_{Fe} = 55.8$ g/mol), the mean mass fraction of metals in the scale on T91 is $w_{M(scale)} = 0.723$. The criterion for transfer of steel constituents is $m_{M(scale)} \neq |\Delta m_M|$, with $m_{M(scale)} < |\Delta m_M|$ and $m_{M(scale)} > |\Delta m_M|$ indicating transfer from the solid phases to the LBE and *vice versa*. The difference ($m_{M(scale)} - |\Delta m_M|$) gives the amount of transferred metal and, after dividing by the exposed surface area, the mass flux of metals between the solid phases and the LBE. Again, the presence of an IOZ causes uncertainties which, in the case of the gravimetric examination, affect the actual value of $w_{M(scale)}$.

The results of the gravimetric analyses on specimens J10 and J12 show that, in the case of J10, the value for $m_{M(scale)}$ (Table 11) is only slightly less than $|\Delta m_M|$ (Table 10). The deviation of $m_{M(scale)}$ from $|\Delta m_M|$ amounts to only 0.3 %, which, if identified with the experimental error, indicates a high accuracy of the gravimetric method with respect to the quantification of the amount of transferred metal and a negligible effect of internal oxidation on $w_{M(scale)}$ for the oxide scale formed on T91 under the experimental conditions. The approximate correspondence between $m_{M(scale)}$ and $|\Delta m_M|$ can be regarded as a confirmation of the less clear findings from the metallographic examinations on specimen J11. In the case of J12, the gravimetric analysis is influenced by the significant error in $|\Delta m_M|$ due to the imperfect pickling procedure chosen for the removal of the oxide scale.

6 Conclusions and recommendations

Three methods of quantifying the degradation (metal recession) of steels exposed to oxygen-containing LBE have been introduced:

(Method A)   Metallographic method to determine the geometric dimensions of sound metal under the light-microscope;

(Method B)   Metallographic method to determine the thickness of different parts of the oxide scale on the steel surface using the light-microscope;

(Method C)   Gravimetric method to determine the mass change after exposure and removal of adherent oxides.

The application of these methods has been demonstrated using cylindrical specimens of martensitic steel T91 that were exposed for 1500 h to stagnant, oxygen-saturated LBE at 550°C. Results for the metal recession following from the three methods coincide with each other within a range of ±3 µm for a mean metal recession of 11 µm. The appropriateness of Method B strongly depends on the growth direction of the oxides that form on the steel surface and has to be proven for the specific material under investigation. Furthermore, the decisive layers of the scale must not spall off (or be eroded) during the exposure. The advantages of Method B over Methods A and C are that no pre-exposure measurements are required, and the results are comparatively accurate when the metal recession is small (short exposure times). The applicability of Method A strongly depends on the precision of the determination of the geometric dimensions of the steel sample before the exposure.

Method C requires that an appropriate procedure for removing the oxide scale from the steel surface is available.

Provided that the initial geometric dimensions, i.e., the diameter in the case of a cylindrical specimen, was measured with sufficient accuracy (e.g., 2-4 µm with the equipment introduced in this report), a main source of error in remeasuring the diameter under the microscope (Method A) is an elliptical distortion due to imperfect metallographic preparation. This error can be significantly reduced when taking the smallest value of a series of measurements as the diameter of sound metal instead of the mean value. Measuring the diameter in pairs of orthogonal diameters helps in identifying an elliptical distortion of the examined cross-section, and increasing the number of diameter measurements on obviously distorted cross-sections improves the accuracy of the smallest diameter. However, the information on the variation of the metal recession due to non-uniform corrosion along the circumference of the specimen (advantage of Method A over Method C) may get lost for a significantly distorted cross-section.

Quantitative information on the transfer of steel constituents between the solid phases (steel and adherent oxides) and the LBE can be obtained when, in addition to the metal recession, the dimensions of the oxide scale are determined. In the presence of an internal oxidation zone (IOZ), the measurements of the thickness of distinguishable parts of the oxide scale under the microscope do not yield reliable quantitative information on this mass transfer, unless the composition of the IOZ (volume fraction, type and composition of precipitated oxides) is also analysed. A rough estimation of the amount of metal transferred from the steel to the LBE is possible, only if specific assumptions about the growth direction of the oxides are fulfilled. The result of the respective gravimetric analysis, i.e., measuring the specimen mass after both stripping adherent LBE off the oxide scale surface and subsequent removal of the oxide scale, is less sensitive to the presence of an IOZ, at least in the case of T91, because the decisive characteristic of the oxide scale (including the IOZ)—the mean mass fraction of metals—does not considerably differ between the IOZ and the oxide layers (consisting of magnetite and (Fe,Cr)-spinel in the case of T91). However, when more than one steel constituent is transferred between the solid phases and the LBE, the determination of the distribution of the overall mass flux of metals on the single steel constituents is only possible if additional information, e.g., from metallographic analyses, is available.

With respect to the successive removal of adherent LBE and the oxide scale, which is necessary for the gravimetric analysis, it is recommended to strip the main part of the LBE off the oxide scale surface by a treatment in hot fat. Remnants of LBE should be removed using half-concentrated nitric acid in an ultrasonic bath. A treatment with nitric acid for about 5 min is suggested, but this time may have to be shortened when considerable amounts of oxide particles flake off. For removing the oxide scale (if present, including an IOZ), an alternate treatment with boiling alkaline potassium permanganate solution and inhibited hydrochloric acid (in an ultrasonic bath at room-temperature) is recommended. In the case of martensitic T91, a pickling procedure consisting of the treatment with

(1) boiling alkaline potassium permanganate solution for 30 min;

(2) inhibited hydrochloric acid for 1 h;

(3) boiling alkaline potassium permanganate solution for 30 min; and

(4) inhibited hydrochloric acid for 10 min

yielded satisfactory results, but especially the duration of the second step may have to be shortened or prolonged depending on the thickness of the IOZ.

Considering the respective benefits of the measurements under the microscope and the gravimetric analysis in the determination of the metal recession and quantification of metal transfer between the solid phases and the LBE, it is suggested to make provisions for both types of methods. This means that at least two specimens of the same material should be used for each exposure time and testing condition, after performing the required pre-exposure measurements.

Acknowledgements

References

1. C. Schroer, Z. Voß, O. Wedemeyer, J. Novotny, J. Konys, "Oxidation of steel T91 in flowing lead-bismuth eutectic (LBE) at 550°C" 7th International Workshop on Spallation Materials Technology, Thun (CH), 2005. *Submitted for publication in J. Nucl. Mater*.

2. D.B. Meadowcroft, J.E. Oakey, "Guidelines for Plant Measurements of High Temperature Corrosion" in Guidelines for Methods of Testing and Research in High Temperature Corrosion, eds. H.J. Grabke, D.B. Meadowcroft (London: The Institute of Materials, 1995) 1-10.

3. J.R. Nicholls, "Discontinuous Measurements of High Temperature Corrosion", *ibid.*, 11-36.

4. G. Müller, G. Schumacher, F. Zimmermann, J. Nucl. Mater. 278, 1(2000) 85-95.

5. C. Schroer, Corros. Sci. 48, 3(2006) 546-563.

6. J. Zhang, N.Li, Oxid. Met. 63, 5/6(2005) 353-381.